

Improved Spatially Coupled Multiuser Superposition Transmission via Constellation Rotation

Min Jiang and Zhongwei Si

Key Laboratory of Universal Wireless Communications, Ministry of Education

Beijing University of Posts and Telecommunications, Beijing, China 100876

Email: {jmin, sizhongwei}@bupt.edu.cn

Abstract—Spatial coupling has been applied in multiple access system in order to obtain higher spectral efficiency, where different users share the same resource blocks by superimposing different data streams with time offsets. In this paper, we introduce constellation rotation into multiuser superposition transmission system for the aim of overcoming the interference between superimposed multiuser and improving the system performance, we make an optimization by maximizing the average mutual information (AMI) to find the optimal angle set. Simulation results show that constellation rotation contributes to improve the system performance and reduce the implementation complexity and the latency. The system with the optimal rotation angle set outperforms the others.

I. INTRODUCTION

With the growing demand, the fifth generation (5G) wireless communication faces many challenges including high spectral efficiency and massive connection. Conventional orthogonal multiple access (OMA) is difficult to meet the demand, and non-orthogonal multiple access (NOMA) [1] catches numerous attractions for its non-orthogonal resource allocation. In NOMA, data streams from different users are allowed to be superimposed, which makes the system achieve higher spectral efficiency. NOMA modulation [2], power allocation and user scheduling [3] are potential research directions to improve system performance.

Spatial graph coupling is a method where a new graph is produced by connecting copies of a protograph randomly. The technique was first applied to construct spatially coupled low-density parity-check (LDPC) codes [4] which proved to reach the same threshold as the maximum a posteriori probability (MAP) decoding threshold of the corresponding LDPC block codes [5]. Recently, applications of the method have been found in multiple access, where different users share the same resource blocks by superimposing different data streams with time offsets. In [6], it has been proved that the spatial coupling achieves the capacity of multiple access channel. Spatial coupling is used in code-division multiple-access (CDMA) in [7] which improves the performance of iterative multiuser detection. A multiple access demodulation with lower complexity is proposed in [8] which obtains the same performance as the others.

Spatially coupled transmission achieves a good performance in terms of high utilization in theory, but in practice, the interference between different data streams of all users is difficult to distinguish only with the help of channel coding. To

solve this problem, constellation rotation is introduced in [9]. Constellation rotation contributes to increase the modulation diversity and is widely used to make a further distinction when data is superimposed. The multi-dimensional sparse code multiple access (SCMA) codebook design with constellation rotation proposed in [10] achieves better performance.

In this paper, we introduce constellation rotation into spatially coupled multiuser superposition transmission. Each data stream is encoded by LDPC codes and transmitted via additive white Gaussian noise (AWGN) channel. During the modulation, different data streams of each user or all data streams of all users are modulated with different constellation rotations. In comparison to the existing methods, we increase the constellation diversity of the superimposed data and make a further distinction between different data streams which can be used by the detector at the receiver. Furthermore, we search for the optimal angle set with the target of maximizing AMI. The spatial coupling is constructed by superimposing the data streams with time offsets. At the receiver, we employ iterative detection and decoding algorithm for data processing. We draw the conclusion that the rotation contributes to the performance improvement in terms of extrinsic information transfer (EXIT) charts and bit error rate (BER) curves.

The rest of this paper is organized as follows. In Section II, the system model of spatially coupled multiuser superposition transmission is introduced. We make elaborated theoretical analysis containing spatial coupling based on constellation rotation, rotation angles optimization and the iterative detection and decoding algorithm in Section III. The simulation results and discussions are represented in Section IV with the help of EXIT curves and BER curves. Finally, Section V summarizes this paper.

II. SYSTEM MODEL

The system model of spatially coupled multiuser superposition transmission in this paper is shown in Fig. 1. We make assumptions that all users have the same numbers of data streams and packages and each data stream is equal-power and independent. To simplify the description, we take $\mathbf{b}_{l,s}$ as an example, which represents the s -th data stream of user l , $l \in \{1, \dots, L\}$, $s \in \{1, \dots, S\}$, and L and S denote the number of user and the number of data streams per user, respectively. At the transmitter, binary information sequence $\mathbf{b}_{l,s} = [\mathbf{b}_{l,s,1}^T, \mathbf{b}_{l,s,2}^T, \dots, \mathbf{b}_{l,s,P}^T]^T$ in P packages is encoded by

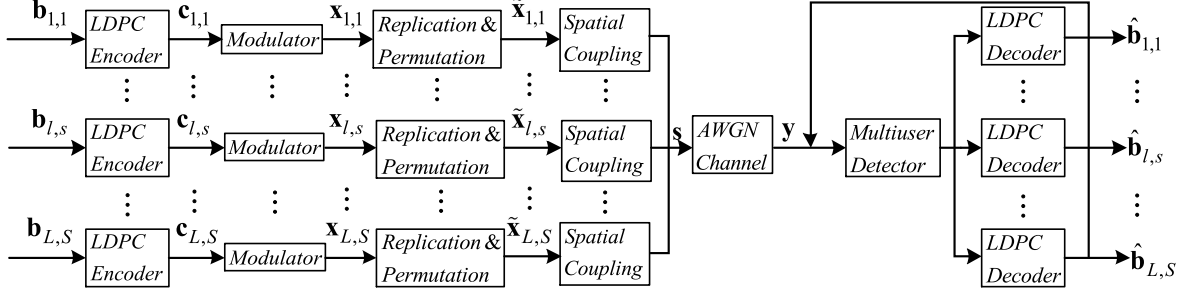


Fig. 1. The system model of spatial coupling multiuser superposition transmission with L users and S data streams per user.

LDPC encoders with code rate $R = K/N$, where sequence $\mathbf{b}_{l,s,p} = [b_{l,s,p,1}, b_{l,s,p,2}, \dots, b_{l,s,p,K}]^T$, $p \in \{1, 2, \dots, P\}$, K is the length of source information in a package and N is the length of the corresponding encoded codeword. In the modulator, the encoded data stream $\mathbf{c}_{l,s}$ is modulated with constellation rotation. The output of the modulator is denoted by sequence $\mathbf{x}_{l,s} = [\mathbf{x}_{l,s,1}^T, \mathbf{x}_{l,s,2}^T, \dots, \mathbf{x}_{l,s,P}^T]^T$, where $\mathbf{x}_{l,s,p} = [x_{l,s,p,1}, x_{l,s,p,2}, \dots, x_{l,s,p,N}]^T$. Then each package of $\mathbf{x}_{l,s}$ is replicated M times and permuted with different interleavers, which produces signal $\tilde{\mathbf{x}}_{l,s}$ composed of $\{\tilde{\mathbf{x}}_{l,s,1}^1, \dots, \tilde{\mathbf{x}}_{l,s,1}^M, \dots, \tilde{\mathbf{x}}_{l,s,P}^1, \dots, \tilde{\mathbf{x}}_{l,s,P}^M\}$. $\tilde{\mathbf{x}}_{l,s}$ is superimposed on other data streams to generate the signal \mathbf{s} when spatial coupling. We define the system described above as a (L, S, P, M) -multiuser spatial coupling structure.

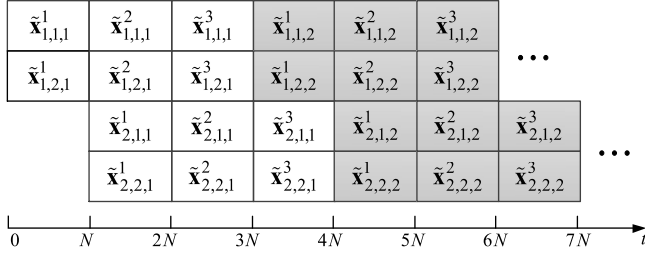


Fig. 2. Coupling of modulated data streams with time offset N in a $(2, 2, P, 3)$ -multiuser spatial coupling structure.

Without loss of generality, we consider the $(2, 2, P, 3)$ -multiuser spatial coupling structure. The spatial coupling procedure is represented in Fig. 2, where each row is a data stream of a user and the packages are transmitted one after another. The block $\tilde{\mathbf{x}}_{l,s,p}^m$ can be denoted as $\tilde{\mathbf{x}}_{l,s,p}^m = \pi_{l,s,p}^m \mathbf{x}_{l,s,p}$, where $\pi_{l,s,p}^m$ is the corresponding interleaver. At time $t = 0$, two data streams of the first user start to transmit. The signal transmitted adds two data streams of the other user after N bit intervals in order.

$$\mathbf{H} = \begin{bmatrix} \pi_{1,1,1}^1 & \dots & \pi_{1,1,1}^M & \dots & \pi_{1,1,P}^1 & \dots & \pi_{1,1,P}^M & \dots \\ \pi_{1,2,1}^1 & \dots & \pi_{1,2,1}^M & \dots & \pi_{1,2,P}^1 & \dots & \pi_{1,2,P}^M & \dots \\ \vdots & \dots & \vdots & \dots & \vdots & \dots & \vdots & \dots \\ \pi_{1,S,1}^1 & \dots & \pi_{1,S,1}^M & \dots & \pi_{1,S,P}^1 & \dots & \pi_{1,S,P}^M & \dots \\ \pi_{2,1,1}^1 & \dots & \pi_{2,1,1}^M & \dots & \pi_{2,1,P}^1 & \dots & \pi_{2,1,P}^M & \dots \\ \pi_{2,2,1}^1 & \dots & \pi_{2,2,1}^M & \dots & \pi_{2,2,P}^1 & \dots & \pi_{2,2,P}^M & \dots \\ \vdots & \dots & \vdots & \dots & \vdots & \dots & \vdots & \dots \\ \pi_{2,S,1}^1 & \dots & \pi_{2,S,1}^M & \dots & \pi_{2,S,P}^1 & \dots & \pi_{2,S,P}^M & \dots \\ \vdots & \dots & \vdots & \dots & \vdots & \dots & \vdots & \dots \\ \pi_{L,1,1}^1 & \dots & \pi_{L,1,1}^M & \dots & \pi_{L,1,P}^1 & \dots & \pi_{L,1,P}^M & \dots \\ \pi_{L,2,1}^1 & \dots & \pi_{L,2,1}^M & \dots & \pi_{L,2,P}^1 & \dots & \pi_{L,2,P}^M & \dots \\ \vdots & \dots & \vdots & \dots & \vdots & \dots & \vdots & \dots \\ \pi_{L,S,1}^1 & \dots & \pi_{L,S,1}^M & \dots & \pi_{L,S,P}^1 & \dots & \pi_{L,S,P}^M & \dots \end{bmatrix} \quad (1)$$

We can also use spatial coupling matrix \mathbf{H} to describe the above procedure. The construction of \mathbf{H} is shown in (1), where $\pi_{l,s,p}^m$ is the permutation matrix of an $N \times N$ unit matrix. Therefore, the signal \mathbf{s} can be described as $\mathbf{s} = \mathbf{H}^T \mathbf{x}$, where $\mathbf{x} = [\mathbf{x}_{1,1,1}^T, \dots, \mathbf{x}_{1,1,P}^T, \dots, \mathbf{x}_{L,S,1}^T, \dots, \mathbf{x}_{L,S,P}^T]^T$. The total load in the system we proposed is shown in (2), which is actually the ratio between rows and columns of \mathbf{H} .

$$Load = \frac{LSPN}{(PM + L - 1)N} = \frac{LSP}{PM + L - 1}. \quad (2)$$

Considering the signal \mathbf{s} is transmitted through the AWGN channel, the received signal \mathbf{y} can be represented as

$$\mathbf{y} = \lambda \mathbf{s} + \mathbf{n}, \quad (3)$$

where λ is the power normalization coefficient, \mathbf{n} is the complex AWGN with zero mean and $\sigma^2/2$ variance for each dimension.

At the receiver, iterative detection and decoding based on message passing algorithm (MPA) is performed. Inner the spatial coupling structure, the extrinsic messages are iteratively exchanged along edges between channel nodes and variable nodes. For the iteration between detector and decoders, which is called outer iteration, the output of the detector is transmitted to the decoders, the outputs of the decoders is used as the input of the detector for the next iteration. Note that each package of a data stream is encoded and decoded individually and the maximum number of the outer iteration is defined as I_{\max} .

III. CONSTELLATION ROTATION IN SPATIAL COUPLING

A. Constellation rotation

For each data stream, the principle of constellation rotation is illustrated in Fig. 3, where the modulated signal is constructed by anticlockwise rotating the standard modulation with a certain angle θ , $\theta \in [0, 180)$.

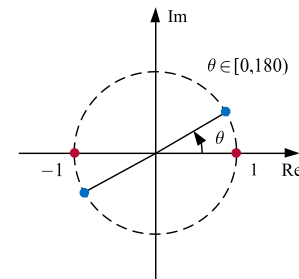


Fig. 3. The constellation rotation of each data stream.

Assuming $\mathbf{x}'_{l,s}$ denotes the BPSK modulated signal of $\mathbf{c}_{l,s}$, $\mathbf{x}'_{l,s} = [\mathbf{x}'^T_{l,s,1}, \mathbf{x}'^T_{l,s,2}, \dots, \mathbf{x}'^T_{l,s,P}]^T$. Then $\mathbf{x}'_{l,s}$ is rotated with angle $\theta_{l,s}$, and $\mathbf{x}_{l,s}$ can be described as

$$\mathbf{x}_{l,s} = e^{i\theta_{l,s}} \mathbf{x}'_{l,s}. \quad (4)$$

B. Spatially coupling based on constellation rotation

To our knowledge, there exists inevitable interference when different signals are superimposed in spatially coupled multiuser superposition transmission. Therefore, we introduce the constellation rotation to make a further distinction between the superimposed signals.

(I) We deal with the interference between different data streams of each user by rotating them with different angles, and there is no difference between users. It diversifies the constellation of the coupled signal \mathbf{s} and contributes to improving the performance of the system theoretically.

(II) To distinguish the interference between different users, we use different angles to modulate all different data streams, which expands the diversity at the cost of increasing the implementation complexity. Experimental results show that the increase in complexity is negligible when compared to the improvement of performance.

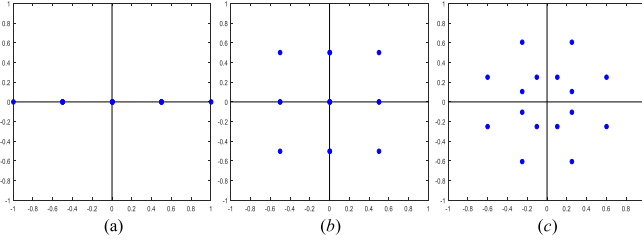


Fig. 4. The constellations of coupled signal \mathbf{s} in $(2, 2, P, S)$ -multiuser spatial coupling system. Rotation angle sets from left to right are $(0, 0, 0, 0)$, $(0, 90, 0, 90)$ and $(0, 30, 60, 90)$, respectively.

We take the $(2, 2, P, S)$ -multiuser spatial coupling system as observation, and the constellations of \mathbf{s} with different rotation angle sets are shown in Fig. 4. As can be seen from the figure, the constellation of \mathbf{s} may contain 16 points when all data streams are modulated with different angles. There exists constellation overlapping when different users use the same rotation rule, we also call this phenomenon constellation aliasing. Nonetheless, both of them obtain higher diversity in constellation compared with the system without any constellation rotation.

When considering constellation, we naturally come up with the minimum Euclidean distance which reflects the interference between constellation points. The minimum Euclidean distance decreases when the diversity of the constellation increases. Therefore, it is necessary to make a trade off between constellation aliasing and interference and search for the optimal rotation angles.

C. Rotation angle optimization

The optimization of rotation angles can be carried out by maximizing AMI between the input \mathbf{S} and the output \mathbf{Y} . The maximum AMI represents the maximum amount

of information about \mathbf{S} that can be conveyed through the channel. Assuming the constellation point set of \mathbf{S} is denoted by $\{\hat{s}_t\}, t \in \{1, 2, \dots, T = 2^{LS}\}$, $\hat{s}_t = a_t + ib_t$, and y represents the element in \mathbf{Y} , $y = u + iv$. The channel transition probability is given as

$$\begin{aligned} p(y|\hat{s}_t) &= \int \int \frac{1}{\pi N_0} e^{-\frac{(u-a_t)^2 + (v-b_t)^2}{N_0}} dudv \\ &= \int \int \frac{1}{\pi N_0} e^{-\frac{|y-\hat{s}_t|^2}{N_0}} dudv, \end{aligned} \quad (5)$$

where N_0 is the noise power spectral density. In order to facilitate the calculation, we assume that $N_0 = 1$. The computational formula of MI is derived as

$$I(\mathbf{S}; \mathbf{Y}) = \sum_{t=1}^T p(\hat{s}_t) \int \int p(y|\hat{s}_t) \log \frac{p(y|\hat{s}_t)}{\sum_{t=1}^T p(\hat{s}_t) p(y|\hat{s}_t)} dudv. \quad (6)$$

As \hat{s}_t occurs with equal probability, we combine (5) and (6), and get

$$\begin{aligned} I(\mathbf{S}; \mathbf{Y}) &= \log T - \\ &\frac{1}{T} \sum_{t=1}^T \int \int \frac{1}{\pi N_0} e^{-\frac{|y-\hat{s}_t|^2}{N_0}} \log \sum_{t'=1}^T e^{-\frac{|y-\hat{s}_{t'}|^2 + |y-\hat{s}_t|^2}{N_0}} dudv. \end{aligned} \quad (7)$$

In our scheme, we traverse all sets of rotation angles when the total number of data streams LS is determined, we use the symmetry to reduce the complexity and stop the traversal the moment the AMI reach its maximum.

D. Iterative detection and decoding

In this section, we describe the process of iterative detection and decoding scheme in detail. During the detection, the LLRs are used as the extrinsic information and passed between nodes given in Fig. 5. The received message of one node along one edge is not allowed to update the message sent from the same edge.

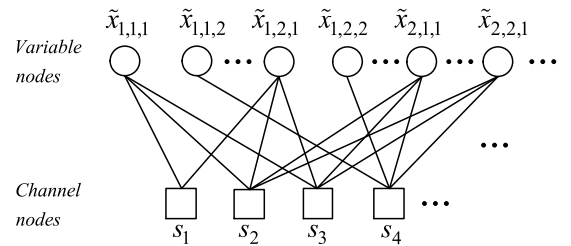


Fig. 5. Factor graph representation of spatial coupling multiple access system, where circles represent variable nodes corresponding to the data blocks in Fig. 2, channel nodes are coupled data and denoted by squares.

Take the edge between variable node $\tilde{x}_{l,s,p}$ and channel node s_t as observation. Set $\xi(l, s, p)$ as the index collection of channel nodes connected with variable node $\tilde{x}_{l,s,p}$ and set $\zeta_t(l, s, p)$ as the index collection of variable nodes connected with channel nodes s_t . Symbol $l_{\tilde{x}_{l,s,p} \rightarrow s_t}$ and $l_{s_t \rightarrow \tilde{x}_{l,s,p}}$ represent the message sent from $\tilde{x}_{l,s,p}$ and s_t , respectively. We initialize $l_{\tilde{x}_{l,s,p} \rightarrow s_t}$ as follows

$$l_{\tilde{x}_{l,s,p} \rightarrow s_t} = \log \frac{p(\tilde{x}_{l,s,p} = +e^{i\theta_{l,s}})}{p(\tilde{x}_{l,s,p} = -e^{i\theta_{l,s}})}. \quad (8)$$

The message updated during the iteration can be write as

$$l_{\tilde{x}_{l,s,p} \rightarrow s_t} = \sum_{t' \in \xi(l,s,p) \setminus t} l_{s_{t'} \rightarrow \tilde{x}_{l,s,p}}, \quad (9)$$

$$l_{s_t \rightarrow \tilde{x}_{l,s,p}} = \log \frac{p(\tilde{x}_{l,s,p} = +e^{i\theta_{l,s}} | s_t, \tilde{\mathbf{x}}^{[t]} \setminus \tilde{x}_{l,s,p})}{p(\tilde{x}_{l,s,p} = -e^{i\theta_{l,s}} | s_t, \tilde{\mathbf{x}}^{[t]} \setminus \tilde{x}_{l,s,p})} \\ = \log \frac{p(s_t | \tilde{\mathbf{x}}^{[t]}, \tilde{x}_{l,s,p} = +e^{i\theta_{l,s}}) p(\tilde{\mathbf{x}}^{[t]} | \tilde{x}_{l,s,p} = +e^{i\theta_{l,s}})}{p(s_t | \tilde{\mathbf{x}}^{[t]}, \tilde{x}_{l,s,p} = -e^{i\theta_{l,s}}) p(\tilde{\mathbf{x}}^{[t]} | \tilde{x}_{l,s,p} = -e^{i\theta_{l,s}})}, \quad (10)$$

where $\tilde{\mathbf{x}}^{[t]}$ denotes the set containing all signals superimposed on the coupled signal s_t . Equation (10) is derived by using Bayes' rule listed below

$$p(x|y) = \frac{p(y|x)p(x)}{p(y)} \propto p(y|x)p(x). \quad (11)$$

The conditional probability density function (pdf) of the coupled signal s_t and the set $\tilde{\mathbf{x}}^{[t]}$ are given separately as

$$p(s_t | \tilde{\mathbf{x}}^{[t]}) = \frac{1}{\sqrt{2\pi}\sigma} \exp\left(-\frac{1}{2\sigma^2} \|s_t - \mathbf{h}^{[t]T} \tilde{\mathbf{x}}^{[t]}\|^2\right), \quad (12)$$

$$p(\tilde{\mathbf{x}}^{[t]} | \tilde{x}_{l,s,p}) = \prod_{(l',s',p') \in \xi(t \setminus (l,s,p))} p(\tilde{x}_{l',s',p'}), \quad (13)$$

where $\mathbf{h}^{[t]}$ is the normalized coefficient vector of $\tilde{\mathbf{x}}^{[t]}$. The symbol $\|\cdot\|$ is modulus operation and a priori probability of $\tilde{x}_{l',s',p'}$ is written as

$$p(\tilde{x}_{l',s',p'}) = \exp\left(\frac{\tilde{x}_{l',s',p'}}{2} l_{\tilde{x}_{l',s',p'} \rightarrow s_t}\right). \quad (14)$$

Substituting (12), (13) and (14) into (10), we get (15) shown on the top of next page, where \max^* operation [11] is defined as follows

$$\max^*(a, b) = \log(\exp(a) + \exp(b)) \\ = \max(a, b) + \log(1 + \exp(-|a - b|)). \quad (16)$$

We define the iterative process from the detector to the decoders as a complete iteration. The message exchanged between the detector and the decoders can be described as

$$l_{out, \tilde{x}_{l,s,p}}^{DEC[i]} = l_{\tilde{x}_{l,s,p}}^{I_{DEC}} - l_{out, \tilde{x}_{l,s,p}}^{DET[i]}, \quad (17)$$

where the symbol on the left side of the equation represents the output of the decoder in the i -th iteration, $i \in \{1, \dots, I_{max}\}$. On the right side, the subtrahend is the LLR of the decoder after I_{DEC} inner iterations and is used for soft decision, the minuend denotes the output of the detector in i -th iteration, initialized as 0 when $i = 1$ and is updated as

$$l_{out, \tilde{x}_{l,s,p}}^{DET[i]} = l_{\tilde{x}_{l,s,p}}^{I_{DET}} - l_{out, \tilde{x}_{l,s,p}}^{DEC[i-1]}, \quad (18)$$

where $l_{\tilde{x}_{l,s,p}}^{I_{DET}}$ is the total LLR received from neighbors of $\tilde{x}_{l,s,p}$ after I_{DET} inner iterations. The symbol $l_{out, \tilde{x}_{l,s,p}}^{DEC[i-1]}$ is the $(i-1)$ -th iterative output of the detector.

IV. SIMULATION RESULTS AND DISCUSSIONS

In this section, we analyze the system performance using EXIT charts and BER curves. The system parameters are

configured as follows. The encoding scheme considered is (3,6)-regular LDPC code with length $N = 1800$ and rate $1/2$.

A. EXIT chart

EXIT chart is a useful tool to track the MI at each iteration in soft-in soft-out (SISO) system, and it provides an excellent prediction on the behavior of the iteration. We use EXIT charts to evaluate the performance of the detector (or decoders) by observing whether it is conducive to increase the output mutual information I_E when the input extrinsic information I_A is given. We produce the EXIT curve with input mutual information and the corresponding output of the detector.

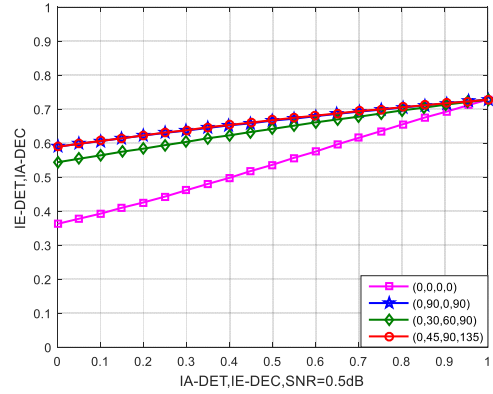


Fig. 6. The EXIT curve of the detector with different rotation angle set in the (2, 2, 5, 2)-multiuser spatial coupling structure with SNR = 0.5dB.

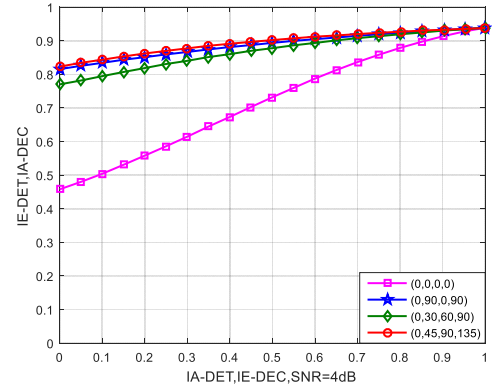


Fig. 7. The EXIT curve of the detector with different rotation angle set in the (2, 2, 5, 2)-multiuser spatial coupling structure with SNR = 4dB.

We take the (2, 2, 5, 2)-multiuser spatial coupling structure as an instance. There are two EXIT curves of detector with different rotation angle set over AWGN channel at SNR = 0.5dB shown in Fig. 6 and SNR = 4dB shown in Fig. 7, respectively. According to the figures above, we reach a conclusion that constellation rotation does contribute to increase the output mutual information of the detector. When we only consider the interference between two data streams of the same user, the optimal rotation angle set is (0, 90, 0, 90), namely, two data streams of each user are orthogonal to each other. That means there exists no interference between certain user's different data streams, but the interference between the

$$\begin{aligned}
l_{s_t \rightarrow \tilde{x}_{l,s,p}} = & \max_{\tilde{\mathbf{x}}^{[t]}} \left(\sum_{(l',s',p') \in \zeta t \setminus (l,s,p)} \frac{\tilde{x}_{l,s,p}}{2} l_{\tilde{x}_{l,s,p} \rightarrow s_t} - \frac{1}{2\sigma^2} \left\| s_t - \mathbf{h}^{[t]T} \tilde{\mathbf{x}}^{[t]} \right\|^2 \right) \\
& \tilde{x}_{l,s,p} = +e^{i\theta_{l,s}} \\
- & \max_{\tilde{\mathbf{x}}^{[t]}} \left(\sum_{(l',s',p') \in \zeta t \setminus (l,s,p)} \frac{\tilde{x}_{l,s,p}}{2} l_{\tilde{x}_{l,s,p} \rightarrow s_t} - \frac{1}{2\sigma^2} \left\| s_t - \mathbf{h}^{[t]T} \tilde{\mathbf{x}}^{[t]} \right\|^2 \right) \\
& \tilde{x}_{l,s,p} = -e^{i\theta_{l,s}}
\end{aligned} \tag{15}$$

two users can not be eliminated and results in the constellation aliasing. When all data streams are taken into account, the diversity of constellation increases. In this case, the optimal rotation angle set we seek out is (0, 90, 45, 135). It can be seen that when the SNR is 0.5dB, the performance of the detector for (0, 90, 45, 135) is almost the same as that for (0, 90, 0, 90). That is to say interference plays a dominant role in the factors affecting the performance rather than diversity. On the contrary, when the SNR is 4dB, the performance of detector is better for (0, 90, 45, 135), which means diversity is the main influencing factor. Anyway, both of them perform better than the system with rotation angle sets randomly selected, such as (0, 30, 60, 90).

B. BER curve

We have demonstrated that the constellation rotation is applicable to any spatial coupling multiuser superposition transmission structure. In this subsection, we only take the (2, 2, 5, 2)-multiuser spatial coupling structure and the (3, 2, 6, 3)-multiuser spatial coupling structure as observations. The optimal rotation angle sets we obtain are (0, 90, 45, 135) and (0, 90, 30, 120, 60, 150), respectively.

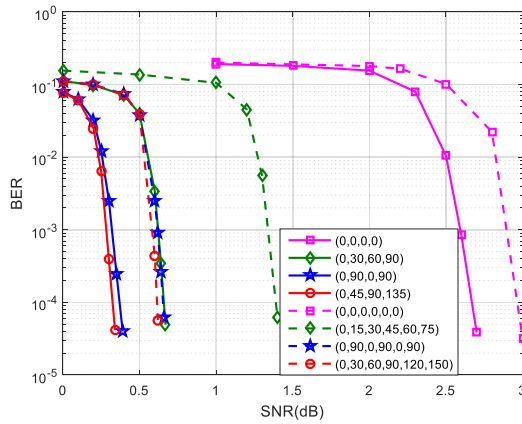


Fig. 8. The average BER curves of different spatially coupled multiuser superposition transmission systems with different rotation angle sets.

We illustrate the average BER curves of the system in Fig. 8, where solid lines and dotted lines represent the systems with the structure (2, 2, 5, 2) and the structure (3, 2, 6, 3), respectively. It can be observed that the system with constellation rotation achieves the better performance indeed and the optimal rotation angle sets we have found out outperform the others in terms of BER performance, which is consistent with the analysis of EXIT charts above. In addition, the performance of

the system with constellation rotation converges faster, which is beneficial to reduce the implementation complexity and the latency of the system.

V. CONCLUSIONS

In this paper, we have introduced constellation rotation into spatially coupled multiuser superposition transmission. We have sought out the optimal rotation angle set by maximizing the AMI. The EXIT charts and BER simulation results verify that the constellation rotation benefits to improve the system performance and reduce the implementation complexity and the latency. The system with the optimal rotation angle set performs better than the others.

REFERENCES

- [1] L. Dai, B. Wang, Y. Yuan, S. Han, C. I. I and Z. Wang, "Non-orthogonal multiple access for 5G: solutions, challenges, opportunities, and future research trends," in *IEEE Communications Magazine*, vol. 53, no. 9, pp. 74-81, September 2015.
- [2] C. Yan, A. Harada, A. Benjebbour, Y. Lan, A. Li and H. Jiang, "Receiver Design for Downlink Non-Orthogonal Multiple Access (NOMA)," 2015 IEEE 81st Vehicular Technology Conference (VTC Spring), Glasgow, 2015, pp. 1-6.
- [3] M. R. Hojiej, J. Farah, C. A. Nour and C. Douillard, "Resource Allocation in Downlink Non-Orthogonal Multiple Access (NOMA) for Future Radio Access," 2015 IEEE 81st Vehicular Technology Conference (VTC Spring), Glasgow, 2015, pp. 1-6.
- [4] D. Truhachev, M. Lentmaier and K. S. Zigangirov, "Mathematical analysis of iterative decoding of LDPC convolutional codes," *Proceedings. 2001 IEEE International Symposium on Information Theory (IEEE Cat. No.01CH37252)*, Washington, DC, 2001, pp. 191.
- [5] M. Lentmaier, A. Sridharan, D. J. Costello and K. S. Zigangirov, "Iterative Decoding Threshold Analysis for LDPC Convolutional Codes," in *IEEE Transactions on Information Theory*, vol. 56, no. 10, pp. 5274-5289, Oct. 2010.
- [6] D. Truhachev, "Universal multiple access via spatially coupling data transmission," 2013 IEEE International Symposium on Information Theory, Istanbul, 2013, pp. 1884-1888.
- [7] K. Takeuchi, T. Tanaka and T. Kawabata, "Performance Improvement of Iterative Multiuser Detection for Large Sparsely Spread CDMA Systems by Spatial Coupling," in *IEEE Transactions on Information Theory*, vol. 61, no. 4, pp. 1768-1794, April 2015.
- [8] C. Schlegel and D. Truhachev, "Multiple Access Demodulation in the Lifted Signal Graph With Spatial Coupling," in *IEEE Transactions on Information Theory*, vol. 59, no. 4, pp. 2459-2470, April 2013.
- [9] R. Zhang and L. Hanzo, "A Unified Treatment of Superposition Coding Aided Communications: Theory and Practice," in *IEEE Communications Surveys & Tutorials*, vol. 13, no. 3, pp. 503-520, Third Quarter 2011.
- [10] D. Cai, P. Fan, X. Lei, Y. Liu and D. Chen, "Multi-Dimensional SCMA Codebook Design Based on Constellation Rotation and Interleaving," 2016 IEEE 83rd Vehicular Technology Conference (VTC Spring), Nanjing, 2016, pp. 1-5.
- [11] R. Hoshyari, F. P. Wathan and R. Tafazolli, "Novel Low-Density Signature for Synchronous CDMA Systems Over AWGN Channel," in *IEEE Transactions on Signal Processing*, vol. 56, no. 4, pp. 1616-1626, April 2008.